Mon. Not. R. astr. Soc. (1991) **248,** 128–138

Optical–infrared studies of the rich cluster of galaxies Abell 370 at $z = 0.37$

Alfonso Aragón-Salamanca, Richard S. Ellis and Ray M. Sharples
Department of Physics, University of Durham, South Road, Durham DH1 3LE

Accepted 1990 August 13. Received 1990 August 9; in original form 1990 July 12

SUMMARY

Using the infrared camera IRCAM on the 3.8-m UK Infrared Telescope we have added new K($\equiv 2$-μm) photometry to existing optical CCD measurements for a complete sample of 53 galaxies with $K < 17.5$ mag in the intermediate-redshift rich cluster Abell 370 ($z = 0.37$). We demonstrate techniques for processing 2-μm images that achieve flatness to 0.04 per cent and a 1 σ surface-brightness detection limit of $\mu_K = 21.5$ mag arcsec^{-2}. The mean optical–infrared colour–magnitude relation for early-type galaxies expected to be members on the basis of both spectroscopy and optical colours, is in excellent agreement with that deduced locally when redshift corrections are applied. In contrast to earlier results, we find no evidence for significant galactic reddening in this direction. However, a large proportion (60 per cent) of red members appear to be $\simeq 0.1$ mag *redder* in R–K than present-day ellipticals, and a high proportion of these have spectroscopic features indicative of the post-starburst phase. Following earlier suggestions, we examine a model whereby a significant fraction of early-type members suffer short-term bursts of star formation. The red excess found in the colour–magnitude relation of Abell 370 can be explained in terms of a contribution by asymptotic giant-branch stars to the post-burst phase, but the high fraction observed seems to imply that virtually all cluster galaxies must suffer this activity at some point in their evolution.

1 INTRODUCTION

Our understanding of the nature of galaxies in distant clusters has improved considerably in recent years due to systematic studies at optical wavelengths. Carefully compiled photometric catalogues (Butcher & Oemler 1978; Butcher, Oemler & Wells 1983) have revealed a systematic excess of blue galaxies associated with rich clusters at modest redshifts ($z \simeq 0.4$) when compared to the number seen in taxonomically similar clusters of the present epoch. Multiple-object spectroscopy of representative clusters at $0.3 < z < 0.5$ (Dressler & Gunn 1983; Couch & Sharples 1987) demonstrated not only that these blue galaxies were indeed cluster members but also that their star formation was likely to have been recently enhanced.

Physical explanations for this enhanced star formation usually point to an environmental process which may be connected with the removal of gas from disc systems destined to become S0 galaxies (*cf.* Gunn 1989). An important development in this context is the claim by MacLaren, Ellis & Couch (1988, hereafter MEC) and Lilly (1987) that recent star formation may have also occurred in some *red* members of the cluster.

MEC found that a significant proportion of optically red galaxies in Abell 370 ($z = 0.37$) displayed an excess of ultraviolet ($\lambda_{\rm rest} \simeq 270$ nm) light consistent with small amounts of ongoing star formation. A similar effect was seen in the more distant cluster 0016+16 (Ellis *et al.* 1985). Available UV data suggest few nearby ellipticals have a significant excess at this wavelength. MEC postulated that such enhanced activity must have been a common feature in a larger fraction of cluster galaxies at $z \sim 0.4$ than the original studies implied, particularly when account is taken of the difficulty of observing such transient effects in the overall population.

By extending the photometry to infrared wavelengths in a number of distant clusters, Lilly (1987) found a discrepancy in the rest-frame V–H colours of otherwise well-behaved early-type galaxies when compared to corresponding values in the nearby Coma cluster. This was attributed to a contribution from massive intermediate-age giant-branch stars, such as might be present if there had been significant star-formation events in the recent history of the distant clusters. Although Lilly sampled over 50 galaxies, the typical number per cluster was small ($\simeq 10$) and so it is not clear what proportion of red galaxies at $z > 0.3$ display this infrared excess. Additionally, the effect claimed ($\simeq 0.1$ mag averaged over all

objects) is only marginally larger than the observational scatter within each cluster.

Our approach in this paper is somewhat different, although our goal is similar, namely to study the red cluster members. Using a significant sample of galaxies in a *single* cluster, and adopting a simple model for the effects of a short-term enhancement in star-formation activity, we hope to use the proportion of galaxies displaying anomalies of the various kinds (UV excess, IR excess, blue optical colours) to estimate the extent of this activity in a given environment. This is an important precursor to any successful physical explanation of the Butcher–Oemler effect.

Abell 370 ($z = 0.37$) was chosen for this study, because of the wealth of accurate optical photometry including the near-ultraviolet from the CCD data of MEC. This cluster is one of the richest examples displaying an excess of blue galaxies and has extensive spectroscopic coverage from the survey of Soucail *et al.* (1988a).

2 OBSERVATIONS AND DATA REDUCTION

An important stimulus for this work has been provided by the advent of imaging cameras at infrared wavelengths. New infrared observations were obtained with the 3.8-m United Kingdom Infrared Telescope (UKIRT) on Mauna Kea during the nights of 1988 October 13 to 16. *K*-band (2.2-μm) images were secured using the 62×58 SBRC InSb IRCAM 1 camera (MacLean *et al.* 1986) in the 1.2-arcsec pixel configuration. Due to the small field of view, three different positions within the cluster were imaged in order to obtain photometry for a significant number of objects. Table 1 gives a log of the observing run.

The on-chip integration time was chosen so that the exposures were background limited without exceeding the well capacity of the chip (957 000 e^-). The *K*-band background, produced by the combination sky + telescope + camera, was typically 12.6 mag arcsec^{-2} and varied with the weather and observing conditions. On-chip exposure times were in the range 10 to 15 s, and a number of single exposures were co-added (~ 25) before storing them on disc as a single image. Each image was taken at a slightly different position (offsets were ~ 2 arcsec) to minimize residual pixel-to-pixel variations in sensitivity and the effect of the several bad pixels. Similar images of several blank areas of the nearby sky were also obtained for flat-fielding purposes.

The response of IRCAM deviates slightly from linearity in the high-count regime, in the sense that the observed count above the bias level is progressively less than it should be. This effect has been calibrated by M. Casali (private communication) and a correction factor was applied to the counts in each pixel of the raw images. This non-linearity does not show any variation with time and is small in the count regime of our frames ($\lesssim 3$ per cent in all cases).

Each co-added image and sky frame was dark (+bias)-subtracted using dark frames obtained with the same on-chip exposures and number of co-additions. As the dark current may change on a time-scale of hours, several dark exposures were obtained during each night and the closest in time was used in every case. We found that, on our particular nights, the large-scale structure of the flat-field changed on time-scales of the order of 10–20 min by as much as ~ 0.4 per cent, which is unacceptable for faint-object photometry with such a high background. It is not therefore possible to create a median flat-field frame with high signal-to-noise ratio which could be useful for the whole night. Thus the 'in-field' chopping technique described by Tyson & Seitzer (1988, and references therein) is unsuitable for our work, since a single 'super-flat' is not valid for all the images. Also, the field is too crowded to allow the use of the flat-fielding method developed by Cowie *et al.* (1990).

After several tests we decided that, for our purposes, the best technique is as follows. Every co-added frame was flat-fielded by dividing it by a normalized sky frame taken close in time. All the images were then registered and scaled to a common sky level (by adding a constant so that the mode of all the frames was the same) and the bad pixels replaced by the mean value of adjacent ones. The final image was then computed as the median of all individual images for each night. This procedure eliminates any remaining defects or cosmic rays and the effect of any faint stars present in the individual sky frames, and produces final images flat to 0.04 per cent. The corresponding 1σ detection limit is $\mu_K = 21.5$ mag arcsec^{-1}. The images of the three different regions were mosaiced by offsetting them and averaging the overlapping areas. A contour plot of this image can be seen in Fig. 1(a). The FWHM image quality is 2.0 arcsec. Note that the giant arc (see Soucail *et al.* 1988b) is clearly visible; photometry for that object has been presented elsewhere (Aragón-Salamanca & Ellis 1989). A contour plot of an optical CCD image of the area (see MEC) is shown in Fig. 1(b) at the same spatial resolution for comparison.

Standard stars from Elias *et al.* (1982) were observed frequently to secure an absolute photometric calibration, and were reduced in a similar way. The zero-points have an internal uncertainty of 0.02 mag. Photometry of the galaxies in Abell 370 was obtained using a 4.8-arcsec-diameter circular aperture centred on each object, and a local sky was estimated from the mode inside similar apertures in carefully chosen blank areas close to each object. Errors were estimated first from the sky variance, and then by comparing photometry from images obtained on different nights and in overlapping areas. Both methods give comparable answers (see Fig. 2), providing a reassuring check on the reproducibility of our photometry. An independent cross-check was provided by comparison with photometry obtained from a very deep image of the giant arc secured with IRCAM 2 during UKIRT service time on 1989 October 29 (see Aragón-Salamanca & Ellis 1990). The measurements for the objects in common agree well within the estimated errors ($\sigma = 0.05$ mag), and the zero-points differ by only 0.006 mag. Since the *K* photometry reaches $K = 17.5$ mag with a pre-

Table 1. Log of observations.

Object	R.A. (1950)	Dec. (1950)	Date	Exposure (s)
Abell 370 (Field 1)	$02^h37^m20^s.0$	$-01°47'34''.9$	1988 October 13/14	6825
			1988 October 15/16	1500
Abell 370 (Field 2)	$02^h37^m20^s.0$	$-01°46'36''.5$	1988 October 14/15	4575
			1988 October 15/16	6000
Abell 370 (Field 3)	$02^h37^m23^s.1$	$-01°47'34''.5$	1988 October 16/17	6750

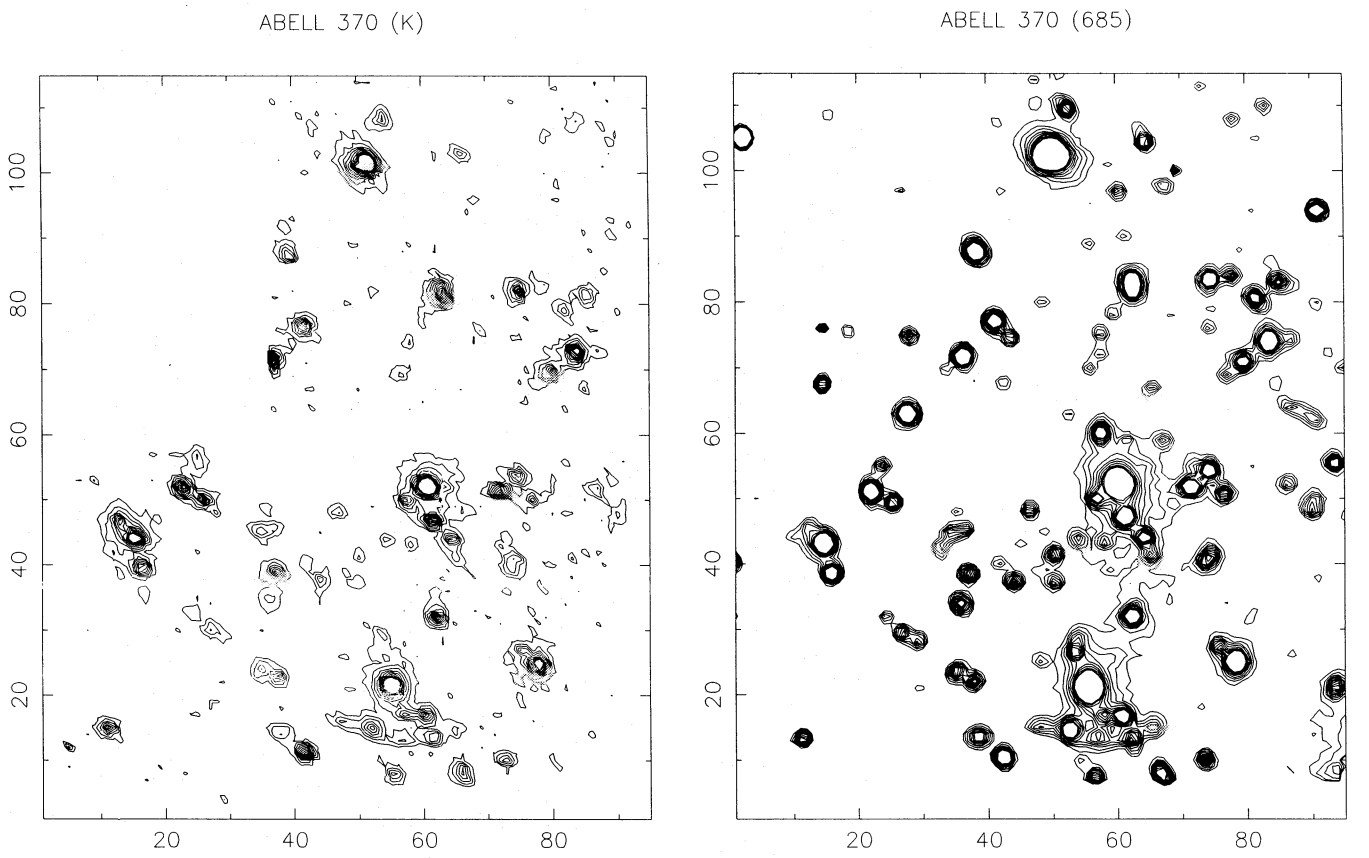

Figure 1. (a) Contour plot of the Abell 370 K-band (2.2-μm) mosaic. The scale is 1.24 arcsec pixel^{-1}. North is up and east is left. The contours follow a linear intensity scale, the lowest corresponding to $\mu_K = 20.7$ mag arcsec^{-2} (2σ above average sky level) and the highest to $\mu_K = 18.2$ mag arcsec^{-2}. Note that part of the north-east quadrant and a strip near $y = 60$ were not imaged. (b) Contour plot of Abell 370 685-band CCD image (see MEC) rebinned to the same pixel scale and covering the same area and equivalent contour levels (from 2σ to 20σ above sky).

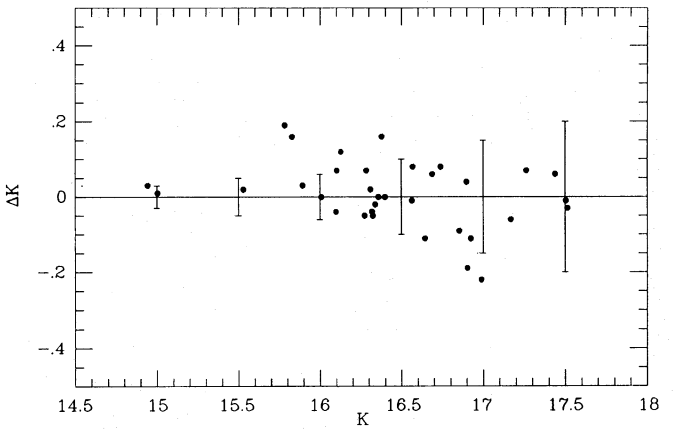

Figure 2. Difference in the K magnitudes measured in different images and overlapping areas as a function of K. The error bars show the 1σ errors estimated from the variance of the sky at different representative K magnitudes. Note that the differences are well within the error bars in most cases.

cision better than 0.2 mag, which is a 5σ detection inside the aperture, we consider our sample 100 per cent complete to this limit.

MEC have obtained broad-band U and several intermediate-band magnitudes (effective wavelengths 418, 502, 685 and 862 nm) for the galaxies in Abell 370. We have combined our K photometry with their optical data (measured with the same 4.8-arcsec-diameter aperture, number 3 in their nomenclature) to obtain long-baseline optical–infrared spectral-energy distributions (SEDs). In order to compare these with data for nearby galaxies (Persson, Frogel & Aaronson 1979, hereafter PFA) we have transformed the 685 magnitudes on to an R (Landolt 1983) scale using two 400-s CCD images obtained with the 1-m Jacobus Kapteyn Telescope at La Palma during a photometric night on 1989 July 8. These images were reduced using standard procedures and calibrated using Landolt photometric standards. Fig. 3 shows the comparison of the R and 685 magnitudes for the brightest objects. It can be seen that a linear transformation with unit slope gives the required accuracy, due to the fact that both pass-bands are quite close. The colour term is proportional to $-0.11(B-V)$ but the colour range in $(B-V)$ of the PFA data is smaller than 0.2 mag, and we thus ignore it. From the La Palma data we conclude that

$$R(3) = 685(3) + 4.468 \pm 0.008. \quad (1)$$

Table 2 contains the final photometric catalogue. Column 1 gives the galaxy number (the numbering scheme follows MEC). Columns 2 and 3 give the K magnitudes (within a 4.8-arcsec-diameter aperture) and the estimated errors. Columns

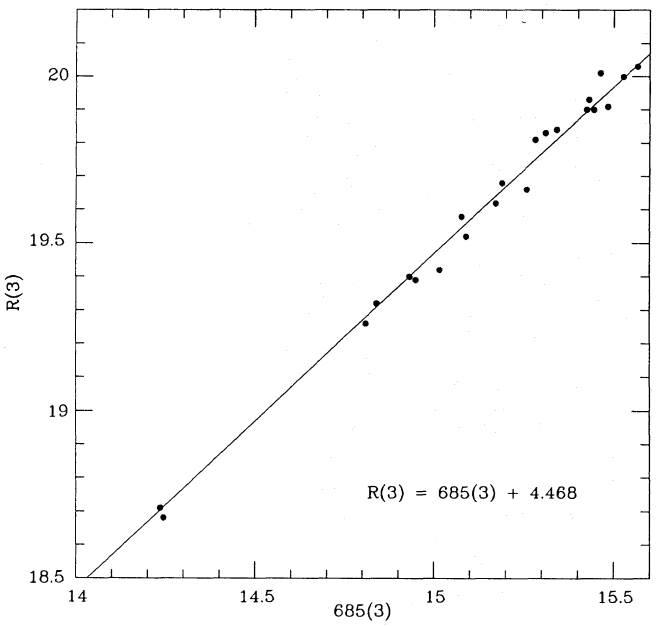

Figure 3. Calibration of 685 magnitudes with R magnitudes for the objects brighter than $R = 20.2$ mag. We used aperture number 3 from MEC (4.8-arcsec diameter). The line shows the relation given by equation (1).

4 and 5 give the $(U–K)$ and $(685–K)$ colours within the same aperture.

3 RESULTS

3.1 The colour–magnitude diagram

Fig. 4 shows the observed $685–K$ colour–magnitude $(C–M)$ relation for Abell 370 cluster members with $K < 17.5$ mag. Spectral classification and cluster membership were determined from the spectroscopic data published by Henry & Lavery (1987), Mellier *et al.* (1988), Newberry, Kirshner & Boroson (1988) and Soucail *et al.* (1988a), when available, and from photometric spectral-energy distribution (SED) classifications from MEC for the remaining galaxies. Some morphological information from high-resolution imaging (Thompson 1988) was also used. Column 6 of Table 2 gives the spectral classification and cluster-membership information for the galaxies in the sample, and column 7 the references. From a total sample of 53 galaxies with $K < 17.5$ mag, 34 (64 per cent) have spectroscopic information. Where comparisons can be made we found an excellent agreement between the spectroscopic and photometric classifications/redshifts for the galaxies in common. Eighty-two per cent of the objects (28 out of 34) agree, and the ones that disagree are mainly late-type galaxies, whose flat spectra make the photometric redshifts very uncertain. As we are mainly interested in early-type galaxies, classification errors from the MEC photometry should have almost no effect on our conclusions. It should be noted that several cross-identification errors are present in MEC's table 3; CCD# 3, 80, 36, 27 and 93 correspond to BO# 58, 62, 55, 105 and 129 respectively, and CCD# 46, 4 and 35 do not have a BO# counterpart. Note also that CCD# 109 was misclassified as an ultraviolet-excess object, since its $U–685$ colour is normal.

Table 2. Photometric catalogue.

CCD#	K	σ_K	(U−685)	(685−K)	Class	References
1	14.95	0.03	4.29	−0.71	E/S0	(1)(2)(4)
107	15.01	0.03	4.22	−0.76	E/S0	(1)(2)(4)
81	15.35	0.04	3.58	−0.63	E/S0+uvx	(1)(2)
20	15.53	0.05	3.55	−0.72	E/S0+uvx	(1)(2)(3)
3	15.78	0.09	4.94	−0.59	E/S0	(1)(2)(4)
29	15.78	0.05	4.14	−0.70	E/S0	(1)(2)(3)
47	15.83	0.06	6.81	−0.90	E/S0	(1)(2)
42	15.90	0.06	4.4	−1.06	E/S0	(1)(2)(4)
32	16.00	0.06	4.18	−0.91	E/S0	(1)(2)
94	16.01	0.06	4.61	−0.68	E/S0	(1)(2)
80	16.01	0.06	4.24	−0.67	E/S0	(1)(2)(3)
22	16.10	0.08	4.14	−0.67	E/S0	(1)(2)
102	16.10	0.07	2.83	−0.93	E/S0+uvx	(1)(2)
105	16.13	0.08	4.26	−0.68	E/S0	(1)(2)
28	16.27	0.08	4.12	−0.51	E/S0	(1)
106	16.29	0.09	4.78	−0.72	E/S0	(1)
36	16.32	0.08	4.15	−1.01	E/S0	(1)(2)
2	16.33	0.08	4.59	−0.64	E/S0	(1)
15	16.34	0.09	4.92	−1.06	E/S0	(1)(2)
68	16.36	0.08	4.01	−0.93	E/S0	(1)(2)
86	16.38	0.08	2.59	−0.63	E/S0+uvx	(1)(2)
4	16.38	0.10	4.91	−0.61	E/S0	(1)(2)
91	16.40	0.09	4.27	−0.39	E/S0	(1)
6	16.49	0.10	4.09	−0.71	E/S0	(1)
14	16.57	0.12	3.61	−1.04	E/S0 (f)	(1)
46	16.57	0.10	2.94	−0.95	E/S0+uvx	(1)(2)
66	16.62	0.10	1.50	−1.60	S	(1)(2)(3)
110	16.65	0.11	4.30	−0.72	E/S0	(1)(4)
90	16.69	0.11	2.24	−0.70	S	(1)(2)(3)
21	16.69	0.12	4.01	−0.60	E/S0	(1)
103	16.74	0.12	2.85	−0.75	E/S0+uvx	(1)
30	16.76	0.12	4.07	−0.36	E/S0	(1)
100	16.80	0.14	2.15	−0.20	S	(1)
26	16.83	0.13	—	−0.83	E/S0	(1)(2)
93	16.85	0.13	2.26	−1.06	S (f)	(1)(3)
27	16.90	0.14	3.60	−1.14	E/S0+uvx	(1)(2)(4)
69	16.91	0.16	2.69	−0.90	E/S0+uvx	(1)(2)
109	16.91	0.14	4.58	−0.72	E/S0	(1)(2)
101	16.93	0.14	1.69	−0.41	S (b)*	(1)(2)
16	16.96	0.15	3.85	−0.81	E/S0	(1)
108	16.99	0.14	1.98	−1.28	S (f)	(1)(3)
88	17.00	0.14	3.49	−0.93	E/S0	(1)
25	17.00	0.15	1.50	−0.59	S	(1)
17	17.17	0.18	3.59	−0.33	E/S0	(1)
258	17.17	0.17	4.83	−0.01	E/S0 (b)	(1)
292	17.26	0.19	2.03	−1.18	S (b)	(1)
19	17.36	0.19	1.66	−1.21	S (f)	(1)(3)
71	17.40	0.22	4.21	−0.87	E/S0	(1)
23	17.41	0.20	3.80	−1.11	E/S0	(1)
70	17.44	0.20	1.97	−1.67	S	(1)(2)(3)(4)(5)
5	17.50	0.24	4.69	−0.85	E/S0	(1)
24	17.51	0.20	2.36	−1.18	S	(1)
45	17.52	0.20	2.41	−0.79	S	(1)(2)(3)(5)

All objects are members unless indicated: (b) background, (f) foreground. E/S0: normal elliptical. E/S0 + uvx: elliptical with ultraviolet excess. S: spiral. (1) MEC (photometry). (2) Soucail *et al.* (1988a) (spectroscopy). (3) Henry & Lavery (1987) (spectroscopy). (4) Newberry, Kirshner & Boroson (1988) (spectroscopy). (5) Thompson (1988) (imaging). *East part of the giant arc.

The red members (objects classified as E and S0 galaxies from spectroscopy and/or narrow-band photometry) show a tight $C–M$ relation, with a scatter of 0.3 mag around the predicted line (see below).

To compare our observed $C–M$ relation with that obtained for nearby galaxies, we have used photometry from PFA, who published *UBVR* and *JHK* magnitudes for nearby E and S0 galaxies using several different aperture sizes. We use their photometry to build a local $C–M$ relation for early-type galaxies, and transform it into our observed $(685–K)$

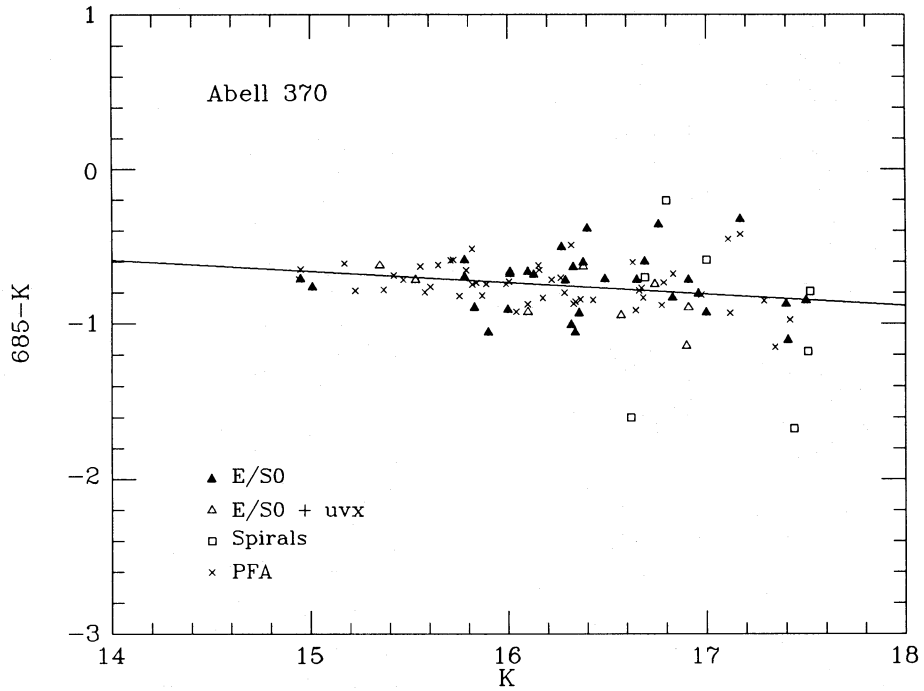

Figure 4. Observed (685−K) versus K C–M diagram for Abell 370 cluster members with $K<17.5$ mag. Filled triangles indicate *normal* E/S0s, open triangles E/S0 with ultraviolet excess and open squares spiral galaxies (see text for membership information and classification). The crosses represent the photometric data for nearby galaxies studied by Persson *et al.* (1979) transformed to the same projected linear aperture and redshift as the cluster (see text for the details of the transformation). The line shows a least-squares fit to the crosses, with a slope of 0.07 mag^{-1}.

versus K diagram at $z=0.37$. The transformation involves redshifting the rest-frame colours, allowing for differences in the responses of the photometric bands, and reducing the photometry to an aperture equivalent to that used in the observations. We transformed the photometry into a 30-kpc metric aperture (4.8-arcsec diameter at $z=0.37$ with $H_0=50$ km s^{-1} kpc^{-1} and $q_0=0.5$. The choice of q_0 has negligible effect in the following discussion due to the fact that the C–M relation is very flat). The Sandage & Visvanathan (1978) growth curve in V and a mean colour gradient of $\Delta(V\text{-}K)/\Delta\log[A/D(0)]=-0.1$ (PFA) were used. Their infrared photometry was transformed from the CIT system to the UKIRT (AAO) system using colour terms published by Bessell & Brett (1988). This correction is very small but was included for consistency.

The K correction in the infrared is very uncertain due to the lack of observed SEDs for early-type galaxies in this wavelength range. Instead of predicting the rest-frame K magnitudes from the observed ones, we have made use of the fact that the K pass-band for a galaxy at $z=0.37$ ($K_{z=0.37}$) corresponds very closely to the H pass-band at $z=0$ ($H_{z=0}$) (see Fig. 5). This allows us to determine a very accurate transformation of $H_{z=0}$ *into* $K_{z=0.37}$ *almost independently* of the object SED (we ignore any small colour gradient in H–K). The transformation was computed by numerical convolution of the filter response curves with several SEDs at the appropriate redshift. The SEDs were determined using broad-band photometry (PFA; Gavazzi & Trincheri 1989) to obtain very low-resolution SEDs of present-day ellipticals and S0s, Bruzual (1983) c-models with different ages (from 3 to 16 Gyr), a giant elliptical model provided by N. Arimoto

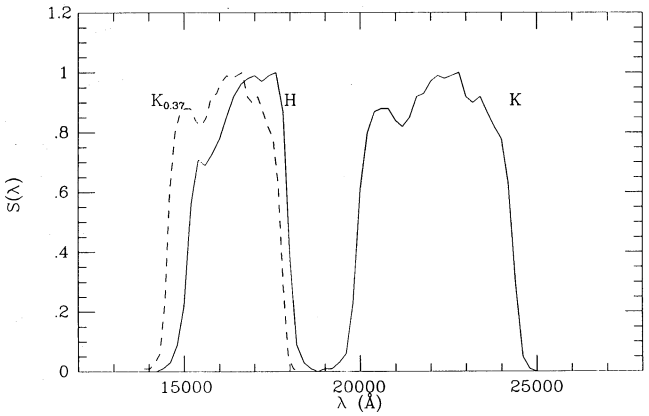

Figure 5. Band-passes of observed H and K (solid line) and rest-frame K at a redshift of 0.37 (dashed line).

(a revised galactic-wind model based on Arimoto & Yoshii 1987) and finally, the airborne spectrophotometry for the K5 giant α-Tau (Strecker, Erickson & Whitteborn 1979, see also Lilly & Gunn 1985). We find

$$H_{z=0}-K_{z=0.37}=0.83\pm0.02, \qquad (2)$$

where the scatter indicates the variation in the four different approaches, which we accept as a suitable transformation for all the ellipticals and S0s.

The prediction of the observed 685 magnitudes (via R) is not as straightforward because the $R_{z=0.37}$ magnitudes have $\lambda_{\rm eff}\sim507$ nm, which lies between the B- and V-bands. How-

ever, detailed early-type galaxy SEDs are available in this region of the spectrum so we can convolve the filter responses with them at the relevant redshifts to get a calibration between $R_{z=0.37}$ *and* $V_{z=0}$ as a function of $(B-V)_{z=0}$. We used the Pence (1976) SEDs for present-day galaxies of different morphological types and also a sequence of spectra used by Couch (1981) to derive a synthetic $C-M$ relation for ellipticals. A linear fit to the resulting transformation gives

$$R_{z=0.37} = V_{z=0} - 0.464 + 0.398(B-V)_{z=0} \quad (3)$$

with an rms scatter of 0.005 mag. This transformation, together with equations (1) and (2), allows us to predict the observed $(685-K)$ versus K $C-M$ diagram for galaxies at $z=0.37$ from the PFA data for nearby galaxies. We estimate that the total uncertainty in the colour transformation is $\lesssim 0.05$ mag. The crosses in Fig. 4 show the transformed PFA data. The straight line is a least-squares fit to these points and has a slope of 0.07 and an rms scatter of 0.16 mag. It agrees very well with the main locus of the observed colours of the E/S0s in A370. The latter are, on average, 0.02 mag redder than the local prediction. This suggests that the extinction towards A370 must be small, *if the local $C-M$ relation is valid for A370*. Using the Savage & Mathis (1979) reddening law and the estimated errors on the transformation, we get a nominal value of $E(B-V)=0.01\pm0.03$, i.e. consistent with zero.

Several independent estimates of the foreground extinction towards A370 are available in the literature. MEC used two different approaches. First they followed the procedure developed by Couch *et al.* (1983) and Ellis *et al.* (1985), which estimates the reddening from the observed SEDs using colours redward of ~ 685 nm. This method gave a very small extinction (they obtained a formal value of $E(B-V)=-0.014\pm0.020$). The second method, described by Couch (1981), uses a study of the colour distribution of field galaxies in the vicinity of A370, and gives $E(B-V)=0.12\pm0.05$. MEC rejected the first estimate (although the method gave results that are reasonably consistent, both from object-to-object and with infrared colours within a given object) and accepted the higher value on the basis of the good agreement between their observed and predicted optical (502–685, 418–685 and U–685 versus R_f) $C-M$ relations when this extinction was applied. On the other hand, the Burstein & Heiles (1982) reddening maps give $E(B-V)\lesssim 0.03$ for this region, and work by Jablonka, Alloin & Bica (1990), using a library of stellar-cluster properties to analyse the spectra of several red galaxies observed by Soucail *et al.* (1988a), suggests a total reddening of $E(B-V)\simeq 0.05$. [It is referred to as 'intrinsic reddening', but, since no foreground-extinction correction was applied, it actually includes the total amount of reddening present (Jablonka, private communication).] Bica (1988), using the same technique, estimates an average *internal* reddening for nearby ellipticals of $E(B-V)\simeq 0.04$, which again implies a very small foreground extinction in this direction $[E(B-V)\simeq 0.01]$. We conclude, therefore, that there is strong evidence in favour of a small reddening towards A370. If the Couch (1981) estimate is correct, either our predicted $C-M$ relation is wrong by ~ 0.2 mag (and we have underestimated the uncertainties of the transformation because there are some poorly understood systematics in the optical–infrared colours), or most of the early-type galaxies in the cluster are too blue in the observed $685-K$ colour by the same amount, which is difficult to understand in the framework of our current knowledge of galaxy evolution (Tinsley 1980; Bruzual 1983; Arimoto & Yoshii 1987). In the rest of the paper we shall assume that the reddening is small (i.e. consistent with zero), as most of the evidence suggests.

The observed rms scatter of the early-type-galaxy colours around the predicted line is 0.3 mag, while the mean observational error is only 0.12 mag. Monte-Carlo simulations of samples with the same error distribution as in Fig. 2 show that this difference is highly significant (to more than a 99 per cent confidence level), so most of the scatter would appear to be intrinsic. A close examination of the distribution of these colours around the predicted $C-M$ relation suggests a bimodal behaviour, especially when looking at objects brighter than $K=17.0$ mag, where the errors are smaller than 0.15 mag. Fig. 6 shows a histogram of the residuals of the observed colours around the predicted line for two different limiting K magnitudes ($K<17.0$ and <16.5 mag). Two peaks, one 0.2 mag bluer and the other 0.1 mag redder than prediction are evident. Whilst this is a small effect, it is potentially very interesting because it might point to some evolutionary differences within the red population. First we estimate the statistical significance of the effect, and then we examine, using evolutionary models, what its cause might be.

Several statistical tests are available to assess the significance of departures from normal distributions, and in particular to study bimodality. First we have followed the method outlined by Lucey, Currie & Dickens (1986, see references therein) which calculates several test statistics for the data points and examines whether these are significantly different from those expected from a normal distribution by constructing (using Monte-Carlo simulations) a large number of control samples (100 000 in our case) with the same population, mean and σ as the data. Not all the normality tests are equally suitable for searching for bimodality in the data. These authors conclude that the kurtosis test (see D'Agostino 1982) is particularly suitable because it is sensitive to the flattening of the distribution. From this test we find that the observed distribution for $K<17.0$ mag would arise from a single Gaussian with a probability of only 0.02 (this probability reduces to 0.01 for $K<16.5$ mag, for which the photometric errors are below 0.1 mag). A second test, specifically sensitive to bimodality, is provided by a one-dimensional version of the Lee statistic (Lee 1979; see Fitchett 1988 for a complete description of the method). In these cases ($K<17.0$ and <16.5 mag), the probability of the distribution arising from a single Gaussian (as opposed to being bimodal) is only 0.002 and 0.004, respectively. The same tests applied to the PFA data show no significant departure from normality: at the same equivalent magnitude limit, the probability of the colour distribution around the main $C-M$ line arising from a single Gaussian is 0.76 from the kurtosis test and 0.75 from the Lee statistic. Since the PFA sample is dominated by field galaxies, it is also desirable to compare our result with objects in a similarly dense nearby environment. Bower, Lucey & Ellis (in preparation) have secured very accurate U, V and K photometry for a sample of E/S0 galaxies in the Coma cluster and have kindly made it available prior to publication. Since they have not measured B and H magnitudes, we cannot perform an identical analysis to the one carried out using the PFA data. However, we have

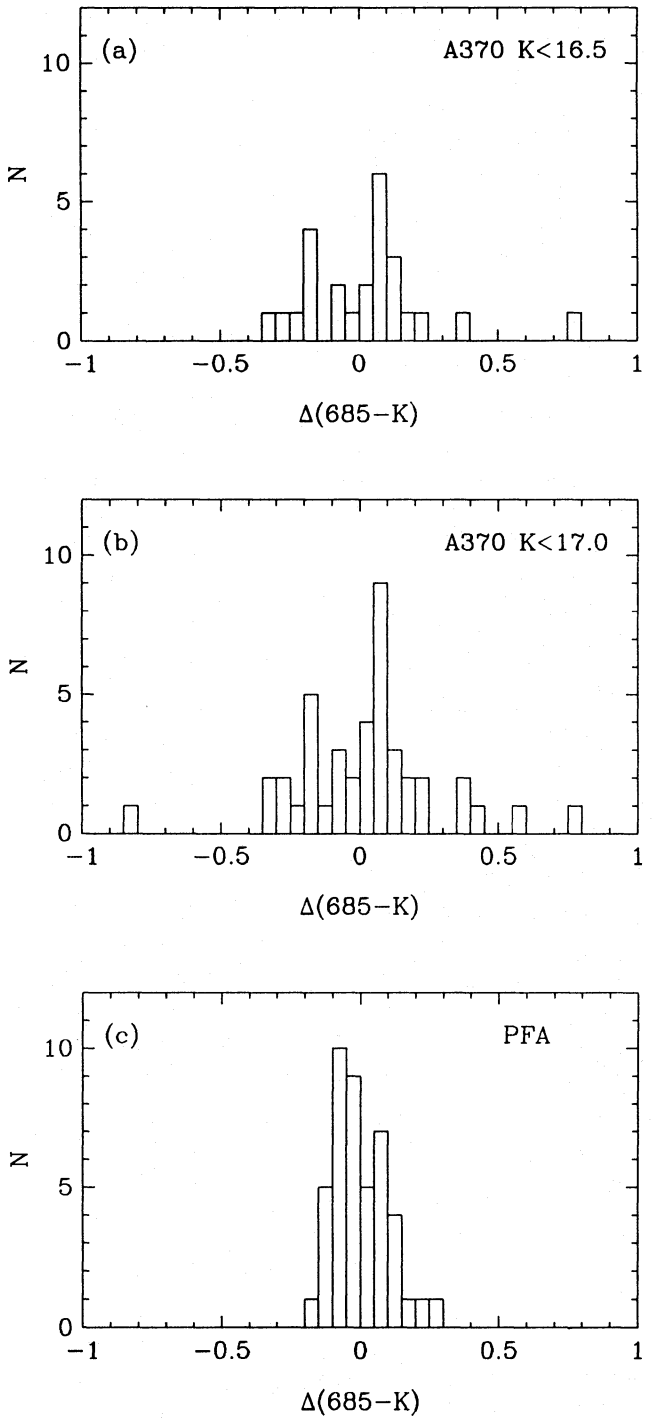

Figure 6. Distribution of the residuals of the observed (685−K) colours around the predicted C–M relation (see text) for (a) the Abell 370 early-type galaxies brighter than $K=16.5$ mag. (b) brighter than $K=17.0$ mag and (c) for the PFA nearby galaxy sample.

analysed the (V–K) versus K C–M relation for the galaxies in their sample and again find no evidence for bimodality [the kurtosis and the Lee tests give probabilities of 0.86 and 0.64, respectively for the (V–K) colour distribution arising from a single Gaussian]. Table 3 summarizes the results of the statistical tests for the different samples.

Table 3. Statistical study of bimodality.

Sample	Colour	Probability	
		Kurtosis test	Lee test
Abell 370 (K<16^m.5)	(685−K)	0.009	0.004
Abell 370 (K<17^m.0)	(685−K)	0.018	0.002
PFA	(685−K)	0.758	0.745
Coma	(V−K)	0.861	0.642

Probabilities are for the colour distributions arising from a single Gaussian.

3.2 The colour–colour diagram

All but one (CCD # 26) of the cluster members included in our $K<17.5$-mag sample have (U–685) colours from MEC, so we can study the (U–685) versus (685–K) colour–colour diagram for an essentially K-magnitude-limited sample (Fig. 7). This diagram can be compared with incomplete versions published by Lilly & Gunn (1985) and Lilly (1987) for C10024+1654 ($z=0.39$). Lilly's diagram shows rest-frame $(U-V)_0$ versus $(V-H)_0$ instead of observed magnitudes, but as we have shown above, the $(685-K)_{z=0.37}$ magnitudes should contain very similar information to the rest-frame $(V-H)_0$. We have made no attempt to K-correct the observed U magnitudes to avoid degrading the data with the uncertainties due to the shapes of the ultraviolet SEDs for different objects, but it should be kept in mind that the U-band is sampling light at ~ 270 nm in the rest-frame.

The structure of both diagrams is remarkably similar, bearing in mind that the present work contains a factor 3 more objects for a single cluster. Three groups of objects populate clearly distinct regions of the diagram. Those classified as *normal* elliptical galaxies form a relatively tight group, especially if we take into account that the C–M relation in both colours will be responsible for some of the scatter because we are sampling a range of 2.5 mag in K, which corresponds to 0.2 mag colour change in (685–K) (with the C–M slope derived above), and 0.3 mag in (U–685) (MEC). This, together with the observational uncertainties in the photometry, accounts for much of the apparent dispersion in colours of these objects in the UV–optical range and some of that observed in the optical–infrared. However, the bimodality of the optical–infrared colours is also responsible for part of the scatter in this axis.

The objects that MEC classified as ultraviolet excess E/S0s form a distinct group on this diagram with (U–685) colours between those of what MEC called *normal* ellipticals and the spirals. The colours of these objects were interpreted by MEC in terms of an elliptical galaxy that has experienced a burst of star formation and is decaying via the post-starburst and UV-excess phase to a normal E/S0. Interestingly, we find that these galaxies show (685–K) colours that belong to both 'red' and 'blue' peaks in the colour–magnitude relation (see Section 4).

Finally, the galaxies classified as *spirals* form a group which has the bluest (U–685) colours, as expected from the SEDs of nearby spirals, but their (685–K) colours span a very wide range, from the reddest E/S0s to ~ 0.5 mag bluer than the bluest ones. This is compatible with the wide range of optical–infrared colours shown by nearby spirals (Aaronson

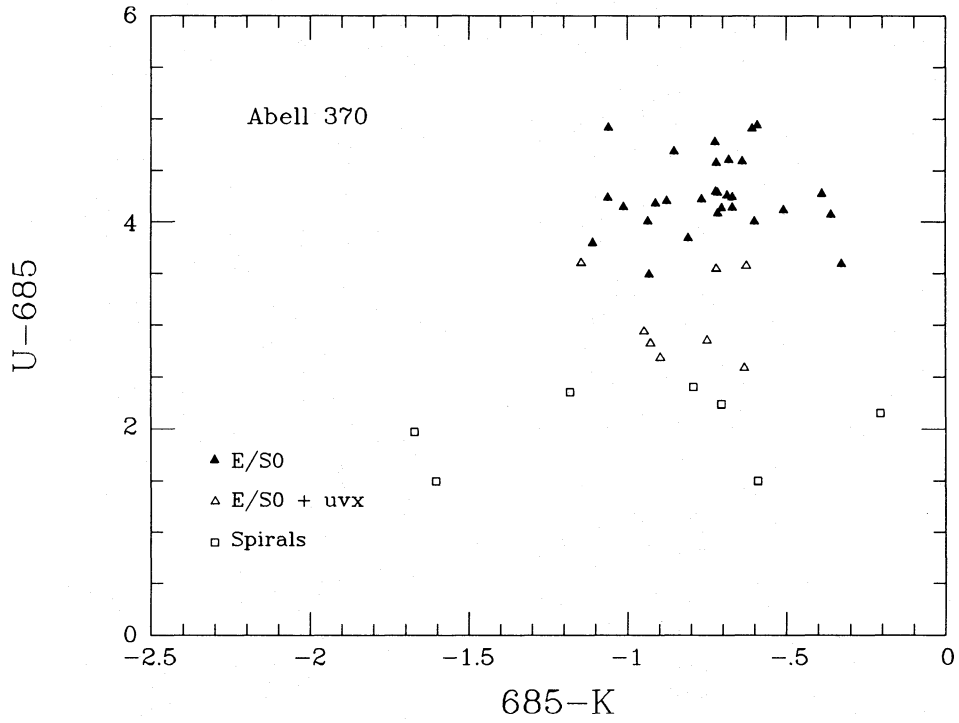

Figure 7. Observed (U–685) and (685–K) colours for Abell 370 members with $K < 17.5$ mag. The symbols are the same as in Fig. 4.

1977, 1978; Gavazzi & Trincheri 1989; see also Lilly & Gunn 1985, fig. 3).

4 ANALYSIS

The physical nature of the bimodality in the optical–infrared C–M diagram of A370 can be understood by close examination of the objects that are in the two peaks. In the following discussion 'red' and 'blue' objects are those members with (685–K) colours redder and bluer than the predicted C–M line, respectively. In the $K < 17.0$-mag sample there are 25 (60 per cent) red and 17 (40 per cent) blue objects according to this definition (10 and 15 in the $K < 16.5$-mag sample). Eight of the 'red' objects (CCD # 3, 20, 22, 29, 80, 81, 94 and 105) and seven of the 'blue' ones (CCD # 15, 32, 36, 42, 47, 68 and 102) have published spectra (Henry & Lavery 1987; Newberry *et al.* 1988; Soucail *et al.* 1988a). Table 4 summarizes the available spectral information. In the 'red' group, five objects show clear evidence of recent star formation in the form of intense Balmer lines and/or UV excess (MEC), and for the other three the data are too poor to reach any conclusion. In the 'blue' group, *none* of the objects with spectroscopy available shows any evidence of departures from a normal early-type-galaxy spectrum, except for the case of CCD # 102. This galaxy lies superimposed on the position of the giant arc, and may be contaminated by the light from this object, which is believed to be the gravitationally lensed image of an intermediate-type spiral galaxy at $z = 0.72$ (Soucail *et al.* 1988b; Aragón-Salamanca & Ellis 1990). The spatial distribution of the galaxies does not seem to be correlated with *red*/*blue* category, although the area imaged in K only reaches a maximum of 1.8 arcmin (0.7 Mpc) away from the cluster centre in the north direction, and considerably less in any other direction. The outer parts of the cluster are therefore not well sampled.

Table 4. Spectroscopic details for cluster members.

CCD#	z (1)	Class.(1)	z (2)	Class.(2)	Comments
			Red objects		
3	~0.37	E/S0	0.466	E	z=0.379; E type?; Mg, H + K? (4)
20	~0.37	E/S0+uvx	0.372	Sa	z=0.370; Red galaxy, Hδ in absorption (3)
22	~0.37	E/S0	0.389	E	—
29	~0.37	E/S0	0.376	E	z=0.375; Red galaxy, Hδ in absorption (3)
80	~0.37	E/S0	0.368	Sa	z=0.378 (3).Balmer lines in absorption?(2)
81	~0.37	E/S0+uvx	0.370	E	Balmer lines in absorption? (2)
94	~0.37	E/S0	0.382	E	—
105	~0.37	E/S0	0.370	Sb?	Very poor spectrum (2).
			Blue objects		
15	~0.37	E/S0	0.383	E	—
32	~0.37	E/S0	0.383	Sa?	Very poor spectrum (2).
36	~0.37	E/S0	0.363	E	—
42	~0.37	E/S0	0.377	Sa/E	z=0.3807; E Type, CN_1, CN_2 (4).
47	~0.37	E/S0	0.378	E	—
68	~0.37	E/S0	0.370	Sa?	Poor spectrum (2).
102	~0.37	E/S0+uvx	0.370	Sb?	Two galaxies superimposed? (2).
			/0.368		Arc contamination?

References as in Table 2. See text for definition of 'red' and 'blue' objects.

The evidence above suggests that some star-formation activity occurred in the recent past in objects that show *red* optical–infrared colours. Although counter-intuitive at first sight, one explanation of the *red* colours is that they are due to the appearance of red asymptotic giant-branch (AGB) stars approximately 10^8 yr after a burst of star formation has occurred (Bica, Alloin & Santos 1990, and references therein). The other red phase found by these authors (due to red supergiants) seems to be too short-lived, lasting only from 7 to 10 Myr, to have a significant statistical effect.

Lilly (1987) argued that galaxies in rich clusters at $z \sim 0.45$ are systematically 0.1 mag redder in the rest frame (V–H)

colour (which is very close to our observed 685–K colour) than local cluster galaxies (Coma). He also interpreted this as an AGB effect, but the conclusions of his work are sensitive to the luminosity evolution correction that he applied, which was based on the evidence found by Lilly & Longair (1984). Our present work is not very sensitive to such evolution because the C–M relation is very flat. In contrast with Lilly, we do not find any evidence for the *average* (685–K) colours of the early-type galaxies in A370 being any different from the colours of present-day E/S0s, as the very good agreement between the predicted and observed C–M diagrams shows. However, the bimodality of the observed C–M diagram strongly suggests that a significant fraction of the early-type galaxies in A370 are undergoing some colour evolution. A quantitative study of the implications of the AGB evolution on the star-formation history of these galaxies is difficult because most evolutionary models for elliptical galaxies usually neglect these late stages of stellar evolution or introduce them without the desired accuracy (Tinsley 1980; Bruzual 1983; Arimoto & Yoshii 1987). However, Wyse (1985) and Chokshi & Wright (1987) have used the theoretical work by Renzini (1981) and Renzini & Buzzoni (1983, 1986) to study the effect of the late stages of stellar evolution (especially the AGB) on existing galaxy-evolution models. Although Frogel, Mould & Blanco (1990) find a deficiency of luminous AGB stars in Magellanic Cloud clusters compared with the theoretical predictions (perhaps due to the effects of mass loss and/or convective overshooting in the late stages of the stellar evolution), the net effect of this result would only be to retard the appearance of the AGB phase (see fig. 15 of Frogel *et al.* 1990) while conserving the order of magnitude of its relative contribution to the integrated bolometric luminosity of the stellar system.

We have used the results of Chokshi & Wright (1987) to model the effect of a burst of star formation on the colours of a normal giant elliptical. We take a galaxy with $M^*_V = -21.77$ ($H_0 = 50$ km s^{-1} Mpc^{-1}), $(B-V)_0 = 0.975$ and $(V-H)_0 = 3.10$ (Tammann, Yahil & Sandage 1980; PFA) and superimpose a burst of star formation that transforms 5, 10 and 20 per cent of the galactic mass into stars. There is no *a priori* information about the time-scale and location of the star formation. It could consist of a global burst that affects a substantial fraction of the galaxy, or one or several smaller bursts. As the time dependence of the star-formation rate (SFR) is unknown, our model is just one of several possibilities. The SFR is assumed to be exponentially decaying with time, with a parameter $\mu = 0.7$ (Bruzual 1983) that corresponds to an e-folding time $\tau = 0.83$ Gyr. A Miller & Scalo (1979) initial mass function (IMF) was assumed. The rest-frame colours of the composite galaxy + burst system are computed as a function of time and then transformed into the observed (685–K) colour using the same procedure applied in Section 3.1. Fig. 8(b) shows the expected change in observed colours produced by such a burst (including the AGB contribution) as a function of the time elapsed after the beginning of the burst. For comparison we have computed a similar model that neglects the late stages of stellar evolution (i.e. a standard Bruzual model) and its predictions are shown in Fig. 8(a).

If we neglect the AGB contribution, the recent star formation produces a blueing of the colours that lasts approximately two e-folding times, decaying into normal galaxy colours afterwards. If the AGB is included, however, the blue

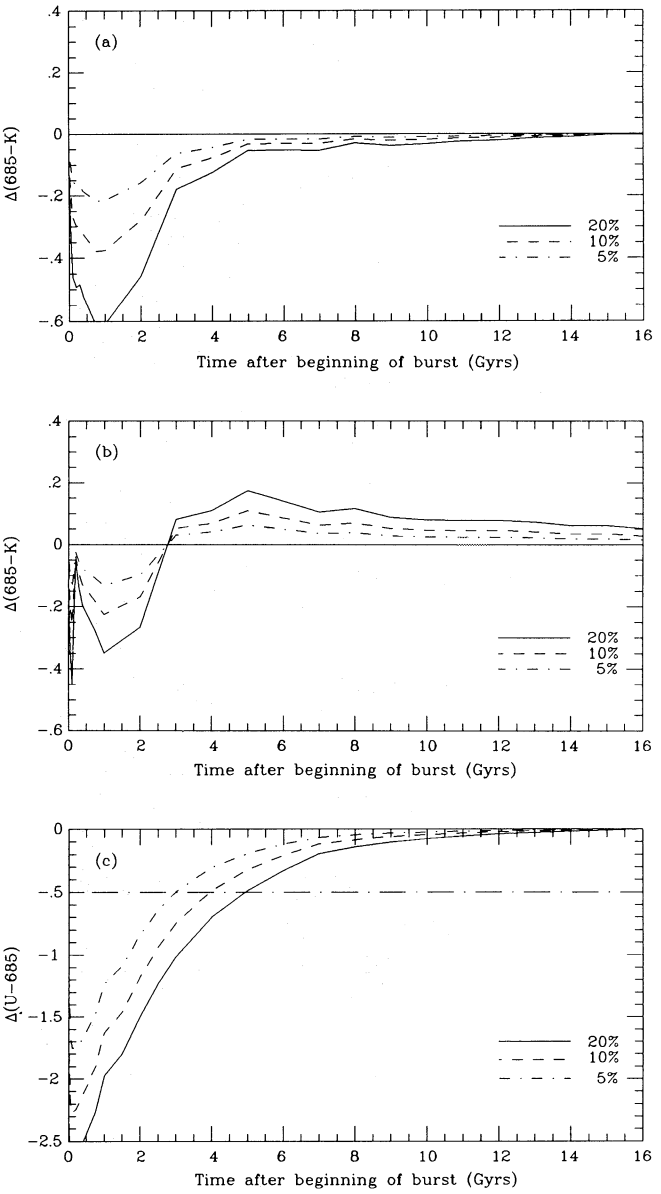

Figure 8. Model predictions of the change in the observed (685–K) colours of a normal giant ellipical at $z = 0.37$ undergoing a burst of star formation that transforms 5, 10 and 20 per cent of its mass into new stars: (a) neglecting the late stages of the stellar evolution (i.e. Bruzual 1983 model), and (b) taking them into account (including AGB). (c) Same as (a) but for (U–685). The horizontal dash-dotted line separates the UV-excess objects from the normal E/S0s according to the MEC definition.

phase is shorter and less pronounced, and is followed by a much longer (several e-folding times) period in which the colours are redder than a passively evolving elliptical before the galaxy reverts to its pre-burst colours. The change in the colours is ~ 0.1 mag when ~ 10 per cent of the mass is transformed into stars, i.e. similar to the observed effect. The expected number of galaxies in the *red* category depends on the SFR time-scale and on the fraction of the galactic mass that is transformed into new stars, but this result seems to fit into the MEC scheme in which a substantial fraction of the early-type galaxies in clusters at intermediate redshifts

undergo bursts of star formation, decaying via the post-starburst and UV-excess phase to normal E/S0s. The red optical–infrared colours in some of these objects are then a manifestation of the burst population passing through an AGB phase. The very high fraction of members that belong to this category (60 per cent) agrees with the relatively long duration of this phase and implies that a large fraction of the galaxies in the cluster must go through it at some point in their evolution. The fact that the objects that MEC classified as E/S0s with ultraviolet excess belong to both *red* and *blue* groups suggests that, if our interpretation of the red optical–infrared colours is correct, the AGB and the ultraviolet phases overlap partly in time. This is possible if the burst of star formation is not instantaneous but has a timescale comparable to the duration of these phases. As can be seen from Fig. 8(c), which shows the evolution with time of the observed (U–685) colours of the galaxy + burst model, we predict that ~ 50 per cent of the galaxies with UV excess should have *red* (685–K) colours, in agreement with the distribution in Fig. 7. More detailed optical spectra of larger samples of galaxies in Abell 370 will be required to explore fully the extent to which this model can explain the wide variety of activity seen in this cluster.

5 CONCLUSIONS

Summarizing our main conclusions.

(i) We have demonstrated the potential of the IRCAM InSb array for precision 2-μm photometry at faint levels. Straightforward processing techniques have allowed us to secure images flat to 0.04 per cent, yielding a surface-brightness detection limit of $\mu_K = 21.5$ mag arcsec^{-2}.

(ii) We have constructed a new catalogue of galaxy photometry for 53 galaxies in the rich cluster Abell 370 ($z = 0.37$). The catalogue is limited at $K = 17.5$ mag and optical–infrared aperture colours have been determined using the work of MacLaren *et al.* (1988). Cluster membership has been determined from earlier spectroscopic and spectrophotometric work. For the red galaxies of interest in this paper, these membership criteria are demonstrated to be very reliable.

(iii) The optical–infrared colour–luminosity (c–L) relation at $z = 0.37$ is closely similar in slope and zero-point to that expected on the basis of present-day observations. The flatness of the relation and reddening uncertainties makes it hard to place strong limits on luminosity evolution over this interval.

(iv) Whilst the mean c–L relation suggests no evolution, on closer examination the scatter is found to be larger than the observational errors and appears to be distinctly non-Gaussian. Interestingly, the spectra of those galaxies with colours redder than the mean line generally show post-starburst-type features, whereas those bluer are largely normal early-type galaxies. This suggests some portion of the scatter in the c–L relation *may* represent the effects of recent star formation.

(v) We demonstrate, using a simple evolutionary model, that a self-consistent star-formation cycle can be constructed whereby an early-type galaxy undergoes a short-term burst of star formation whose post-burst phase may drive it to the red section of the c–L relation via the contribution of asymptotic giant-branch (AGB) stars. The size and duration of the AGB effect is broadly compatible with earlier explanations for the blue bursting population and the ultraviolet-excess ellipticals, but the predominance of this effect suggests that the bulk of the galaxy population in Abell 370 must have suffered this activity at some time and that it is not restricted to recently arrived galaxies destined to form the less-substantial S0 population.

ACKNOWLEDGMENTS

The authors thank Dr J. Lucey and Dr M. Fitchett for their help with the study of bimodality and for providing the software to carry out the statistical tests. R. Bower and J. Lucey provided the photometry of Coma galaxies prior to publication the authors also thank Dr A. Pickles for his useful comments. AAS acknowledges the Physics Department of the University of Durham and SERC for financial support.

REFERENCES

Aaronson, M., 1977. *PhD thesis*, Harvard University.
Aaronson, M., 1978. *Astrophys. J.*, **221,** L103.
Aragón-Salamanca, A. & Ellis, R. S., 1990. In: *The Toulouse Workshop on Gravitational Lenses*, p. 288, eds Mellier, Y., Soucail, G. & Fort, B., Springer-Verlag, Berlin.
Arimoto, N. & Yoshii, Y., 1987. *Astr. Astrophys.*, **173,** 23.
Bessell, M. S. & Brett, J. M., 1988. *Publs astr. Soc. Pacif.*, **100,** 1134.
Bica, E., 1988. *Astr. Astrophys.*, **195,** 176.
Bica, E., Alloin, D. & Santos Jr., J. F. C., 1990. *Astr. Astrophys.*, **235,** 103.
Bruzual, G., 1983. *Astrophys. J.*, **273,** 105.
Burstein, D. & Heiles, C., 1982. *Astr. J.*, **87,** 1165.
Butcher, H. & Oemler, A., 1978. *Astrophys. J.*, **219,** 18.
Butcher, H., Oemler, A. & Wells, D. C., 1983. *Astrophys. J. Suppl.*, **52,** 183.
Chokshi, A. & Wright, E. L., 1987. *Astrophys. J.*, **319,** 44.
Couch, W. J., 1981. *PhD thesis,* Australian National University.
Couch, W. J. & Sharples, R. M., 1987. *Mon. Not. R. astr. Soc.*, **229,** 423.
Couch, W. J., Ellis, R. S., Godwin, J. & Carter, D., 1983. *Mon. Not. R. astr. Soc.*, **205,** 1287.
Cowie, L. L., Gardner, J. P., Lilly, S. J. & McLean, I., 1990. *Astrophys. J.*, **360,** L1.
D'Agostino, R. B., 1982. In: *Encyclopedia of Statistical Sciences*, Vol. 2, p. 315, eds Kotz, S. & Johnson, N., Wiley & Sons, New York.
Dressler, A. & Gunn, J. E., 1983. *Astrophys. J.*, **270,** 7.
Elias, J. H., Frogel, J. A., Mathews, K. & Neugebauer, G., 1982. *Astr. J.*, **87,** 1029.
Ellis, R. S., Couch, W. J., MacLaren, I. & Koo, D. C., 1985. *Mon. Not. R. astr. Soc.*, **217,** 239.
Fitchett, M., 1988. *Mon. Not. R. astr. Soc.*, **230,** 161.
Frogel, J. A., Mould, J. & Blanco, V. M., 1990. *Astrophys. J.*, **352,** 96.
Gavazzi, G. & Trincheri, G., 1989. *Astrophys. J.*, **342,** 718.
Gunn, J. E., 1989. In: *The Epoch of Galaxy Formation*, p. 167, eds Frenk, C. S., Ellis, R. S., Shanks, T., Heavens, A. F. & Peacock, J. A., Kluwer, Dordrecht.
Henry, J. P. & Lavery, R. J., 1987. *Astrophys. J.*, **323,** 473.
Jablonka, P., Alloin, D. & Bica, E., 1990. *Astr. Astrophys.*, **235,** 22.
Landolt, A. U., 1983. *Astr. J.*, **88,** 439.
Lee, K. L., 1979. *J. Am. Stat. Assoc.*, **74,** 708.
Lilly, S. J., 1987. *Mon. Not. R. astr. Soc.*, **229,** 573.
Lilly, S. J. & Longair, M. S., 1984. *Mon. Not. R. astr. Soc.*, **211,** 833.

Lilly, S. J. & Gunn, J. E., 1985. *Mon. Not. R. astr. Soc.,* **217,** 551.
Lucey, J. R., Currie, M. J. & Dickens, R. J., 1986. *Mon. Not. R. astr. Soc.,* **221,** 453.
MacLaren, I., Ellis, R. S. & Couch, W. J., 1988. *Mon. Not. R. astr. Soc.,* **230,** 249.
MacLean, I. S., Chuter, T. C., MacCaughrean, M. J. & Rayner, J. T., 1986. *Proc. SPIE,* **627,** 430.
Mellier, Y., Soucail, G., Fort, B. & Mathez, G., 1988. *Astr. Astrophys.,* **199,** 13.
Miller, G. E. & Scalo, J. M., 1979. *Astrophys. J. Suppl.,* **41,** 513.
Newberry, M. V., Kirshner, R. P. & Boroson, T. A., 1988. *Astrophys. J.,* **335,** 629.
Pence, W. D., 1976. *Astrophys. J.,* **203,** 39.
Persson, S. E., Frogel, J. A. & Aaronson, M., 1979. *Astrophys. J. Suppl.,* **39,** 61.
Renzini, A., 1981. *Ann. Phys.,* **6,** 87.
Renzini, A. & Buzzoni, A., 1983. *Mem. Soc. Astr. Ital.,* **54,** 739.
Renzini, A. & Buzzoni, A., 1986. In: *Spectral Evolution of Galaxies*, p. 195, eds Chiosi, C. & Renzini, A., Reidel, Dordrecht.
Sandage, A. & Visvanathan, N., 1978. *Astrophys. J.,* **223,** 707.
Savage, B. D. & Mathis, J. S., 1979. *Ann. Rev. Astr. Astrophys.,* **17,** 73.
Soucail, G., Mellier, Y., Fort, B. & Cailloux, M., 1988a. *Astr. Astrophys. Suppl.,* **73,** 471.
Soucail, G., Mellier, Y., Fort, B., Mathez, G. & Cailloux, M., 1988b. *Astr. Astrophys.,* **191,** L19.
Strecker, D. W., Erickson, E. F. & Witteborn, F. C., 1979. *Astrophys. J. Suppl.,* **41,** 501.
Tammann, G. A., Yahil, A. & Sandage, A., 1980. *Astrophys. J.,* **234,** 775.
Thompson, L. A., 1988. *Astrophys. J.,* **324,** 112.
Tinsley, B. M., 1980. *Fundam. Cosmic Physics,* **5,** 287.
Tyson, J. A. & Seitzer, P., 1988. *Astrophys. J.,* **335,** 552.
Wyse, R. F. G., 1985. *Astrophys. J.,* **299,** 593.